1964.
(24) K. D. Reppond, Ph.D. Dissertation, University of Arkansas, Fayetteville, Ark., 1974.
(25) R. C. Williams and J. W. Taylor, *J. Am. Chem. Soc.*, **96**, 3721 (1974); **95**, 1710 (1973).
(26) (a) M. J. Stern and M. Wolfsberg, *J. Pharm. Sci.*, **54**, 849 (1965); (b) M. Wolfsberg and M. J. Stern, *Pure Appl. Chem.*, **8**, 325 (1964).
(27) "Table of Interatomic Distances and Configurations in Molecules and Ions", *Chem. Soc., Spec. Publ.*, **No. 11, 18** (1958, 1965).
(28) (a) E. B. Wilson, Jr., J. C. Decius, and P. C. Cross, "Molecular Vibrations", McGraw-Hill, New York, N.Y., 1955, pp 175–176; (b) G. Herzberg, "Molecular Spectra and Molecular Structure", Part II, "Infrared and Raman Spectra and Polyatomic Molecules", Van Nostrand, Princeton, N.J., 1945; (c) J. H. Schachtschneider and R. G. Snyder, *Spectrochim. Acta*, 19, 117 (1963); R. G. Snyder and J. H. Schachtschneider, *ibid.*, **21**, 169 (1965); *J. Mol. Spectrosc.*, **30**, 290 (1969).
(29) L. Pauling, *J. Am. Chem. Soc.*, **69**, 542 (1947); the coefficient of 0.30 listed in the text is a revised value (from 0.26) obtained by least-squares fit to data in ref 27.
(30) R. M. Badger, *J. Chem. Phys.*, **2**, 128 (1934); **3**, 710 (1935).
(31) H. S. Johnston, "Gas Phase Reaction Rate Theory", Ronald Press, New York, N.Y., 1966, Chapter 4.
(32) D. R. Herschbach and V. W. Laurie, *J. Chem. Phys.*, **35**, 458 (1961).
(33) Equation 6 takes into account approximately the observed variations in angle bending force constants with changes in bond angle and bond order for certain hydrocarbons (L. B. Sims, J. C. Wilson, and E. C. Parton, unpublished results). Other evidence has been adduced to support the contention that bending force constants decrease as the angle increases, other things being equal; see L. S. Bartell, *Inorg. Chem.*, **9**, 1594 (1970); R. J. Gillespie and R. S. Nyholm, *Q. Rev., Chem. Soc.*, 11, 339 (1957); R. R. Holmes, Sr., R. M. Dieter, and J. A. Golen, *Inorg. Chem.*, **8**, 2612 (1969).
(34) For S_N2 and E2 models, the equation $F_\theta = g_\theta(n_i n_f)F_\theta^\circ$ gives better agreement between calculated and experimental deuterium isotope effects.
(35) M. J. Stern and M. Wolfsberg, *J. Chem. Phys.*, **45**, 2618 (1966).
(36) W. D. Gwinn, *J. Chem. Phys.*, **55**, 477 (1971).
(37) J. Bigeleisen, *J. Chem. Phys.*, **17**, 675 (1949); J. Bigeleisen and M. G. Mayer, *ibid.*, **15**, 261 (1947).
(38) O. Redlich, *Z. Phys. Chem., Abt. B*, **28**, 371 (1935); E. Teller, 1934, quoted by W. R. Angus, C. R. Bailey, J. B. Hale, C. K. Ingold, A. H. Leckie, C. G. Raisin, J. W. Thompson, and C. L. Wilson, *J. Chem. Soc.*, 971 (1936).
(39) A. J. Kresge, N. N. Lichtin, K. N. Rao, and R. E. Weston, Jr., *J. Am. Chem. Soc.*, **87**, 437 (1965).
(40) J. Bron and J. B. Stothers, *Can. J. Chem.*, **47**, 2506 (1969).
(41) T. H. Cromartie and C. G. Swain, *J. Am. Chem. Soc.*, **98**, 545 (1976).
(42) W. J. Albery and B. H. Robinson, *Trans. Faraday Soc.*, **65**, 1623 (1969).
(43) C. G. Swain and R. F. W. Bader, *Tetrahedron*, **10**, 182 (1960).
(44) J. D. Bernal and R. H. Fowler, *J. Chem. Phys.*, 1, 515 (1933).
(45) Bond energies were calculated by an equation given by Johnston in ref 31, $E = E_s(n_{Cl\text{-}H})^p$, with $E_s = 102.1$ kcal/mol and $p = 0.914$.
(46) R. A. Howald, *J. Am. Chem. Soc.*, **82**, 20 (1960). The isotope effect for this hypothetical equilibrium was obtained by dividing the chlorine isotope effect obtained for the equilibrium of hydrogen chloride partitioning between the gas phase and slightly aqueous acetic acid by the reduced partition function expression (VP·EXC·ZPE) for hydrogen chloride gas.
(47) J. M. Harris, *Prog. Phys. Org. Chem.*, 11, 89 (1974).
(48) V. Gold, *J. Chem. Soc., Faraday Trans. 1*, 1611 (1972).
(49) W. von E. Doering and H. H. Zeiss, *J. Am. Chem. Soc.*, **75**, 4733 (1953).
(50) A. Fry, *Pure Appl. Chem.*, **8**, 409 (1964).

Intramolecular General Base Catalysis of Schiff Base Hydrolysis by Carboxylate Ions

R. H. Kayser and R. M. Pollack*

Contribution from the Laboratory for Chemical Dynamics, Department of Chemistry, University of Maryland Baltimore County, Baltimore, Maryland 21228.
Received September 27, 1976

Abstract: The mechanism of the hydrolysis of a series of Schiff bases (**2**) derived from cyclohexene-1-carboxaldehyde (**1**) and various amines has been examined in aqueous solution. A correlation of the log of the rate of water attack ($k_1^{H_2O}$) with the Schiff base pK_a (slope = −0.98) shows large rate enhancements (60-fold) in $k_1^{H_2O}$ for Schiff bases derived from glycine (**2e**) and aspartic acid (**2g**), and a smaller acceleration (fivefold) for the β-alanine derivative (**2f**). The rate accelerations for **2e–g** are attributed to intramolecular general base catalysis of water attack by the internal carboxyl groups. Brønsted plots for the intermolecular general-base-catalyzed attack of water permitted the calculation of effective concentrations of the internal bases for **2e** (30 M) and **2f** (1 M). The pH–rate profiles for the hydrolysis at low pH, where carbinolamine breakdown is rate limiting, are incompatible with a simple two-step mechanism for Schiff base hydrolysis. Rather, these results, along with kinetic and structure–reactivity data, suggest that carbinolamine breakdown occurs via two concurrent pathways involving zwitterionic and protonated carbinolamine intermediates, respectively.

The intermediacy of a Schiff base in the catalytic action of several enzymes[1-10] has generated a great deal of interest in the mechanism of formation and hydrolysis of these compounds. Although these reactions have been investigated in great detail in model systems,[11] the mechanism by which enzymatic Schiff bases are formed and hydrolyzed is still incompletely understood. Even though the interconversion of many simple Schiff bases with the corresponding carbonyl compounds is very rapid,[12-14] it is often several orders of magnitude too slow to account for the corresponding enzymatic processes.[15] In a previous report[18] we demonstrated that general base catalysis of Schiff base hydrolysis by a carboxylate ion in a relatively nonpolar solvent mixture (dioxane–water) is exceedingly efficient, and we suggested that enzymatic Schiff base hydrolysis might be accelerated by a carboxylate ion acting as a general base at an apolar active site. In order to further evaluate this possibility, we wished to determine whether an internal carboxylate ion could efficiently catalyze Schiff base hydrolysis. Observation of intramolecular catalysis of this reaction would further demonstrate the feasibility of our proposal. In this report we describe the hydrolysis of a series of Schiff bases derived from cyclohexene-1-carboxaldehyde (**1**). Several of these Schiff bases (**2e–g**) have internal carboxylate ions, enabling us to assess the existence of intramolecular catalysis by these groups.

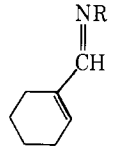

2a, R = $CH_2CH_2CH_3$ **e**, R = $CH_2COO^-K^+$
b, R = CH_2CH_2OH **f**, R = $CH_2CH_2COO^-K^+$
c, R = CH_2CF_3 **g**, R = $CH(COO^-Na^+)CH_2COO^-Na^+$
d, R = CH_2CONH_2

Results

The series of cyclohexene-1-carboxaldehyde Schiff bases **2a–g** were synthesized by mixing the aldehyde (**1**) with the

Table I. Rate Constants for Nucleophilic Attack in the Hydrolysis of **2a–g**[a]

Schiff base	pK_a[b]	$10^{-3}k_1^{H_2O}$, s^{-1}	$10^{-4}k_1^{OH^-}$, $M^{-1}s^{-1}$	k_1^{cat}, $M^{-1}s^{-1}$			
				$ClAcO^-$	AcO^-	$H_2PO_4^{2-}$	Borate
2a	8.34 ± 0.03	0.109	0.68 ± 0.02		8.8 ± 0.5	6.7 ± 0.4	
	(8.32 ± 0.04)	± 0.004			× 10^{-4}	× 10^{-3}	
2b	7.49 ± 0.02	0.628	3.54 ± 0.24	~10^{-3}	5.4 ± 0.1	4.2 ± 0.3	
	(7.51 ± 0.04)	± 0.048			× 10^{-3}	× 10^{-2}	
2c	4.36 ± 0.02	720	62.6 ± 1.4		~2	10.8	120
		± 80				± 0.8	± 10
2d	5.81 ± 0.02	41.3	13.8 ± 0.6	~0.03	0.12	0.99	
		± 1.4			± 0.01	± 0.06	
2e	7.57 ± 0.02	36.8	2.04 ± 0.04		0.011	0.083	
	(7.62 ± 0.05)	± 0.6			± 0.003	± 0.003	
2f	7.76 ± 0.03	2.0 ± 0.1	1.8 ± 0.1		2.5 ± 0.3	0.0181	
					× 10^{-3}	± 0.0005	
2g	7.64 ± 0.02	32.0	0.823			0.046	
		± 0.7	± 0.033			± 0.002	

[a] Measured at 25 °C at ionic strength 1.0 (NaCl) from analysis of eq 2a. All errors are standard deviations. [b] Values in parentheses from kinetic data; other pK_a values determined spectrally.

appropriate amine at room temperature. The liquid Schiff bases (**2a–c**) were purified by preparative GLC or vacuum distillation, while the solid compounds (**2d–g**) were purified by recrystallization. All compounds gave spectra and elemental analysis consistent with the α,β-unsaturated Schiff base structure (**2**).

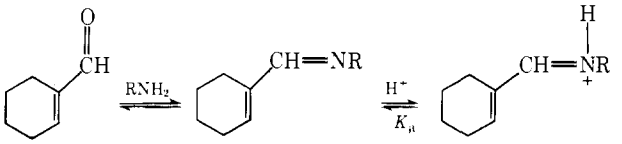

1 2 2 H^+

A bathochromic shift of the absorption maxima in the uv spectra of **2a–g** (from ca. 235 to ca. 260 nm) occurs in acidic solution. Such a shift is consistent with protonation of the imino nitrogen of **2** to give the conjugate acid, $2H^+$.[19] Ionization constants for $2H^+$ were calculated using spectrophotometric methods (and also, in some cases, using kinetic data) as described in the Experimental Section and are shown in Table I.

The hydrolysis of all seven Schiff bases was investigated over a wide pH range (generally 0–12) at 25.0 °C (μ = 1.0). The product was identified spectrophotometrically. Ultraviolet spectra taken after completion of the reaction (at several pHs) were identical with spectra of **1** obtained under the reaction conditions. Routine checks of infinity absorbances of the kinetic runs indicated greater than 90% conversion of **2** to **1** in all cases. Reaction rates were monitored either by observing the decrease in absorbance at 260 nm due to loss of the protonated Schiff base or, under conditions where the Schiff base is largely unprotonated, by following the change in absorbance at 230–235 nm. Excellent first-order kinetics were obtained in all cases. The observed pseudo-first-order rate constants extrapolated to zero buffer concentration (k_{obsd}^0) are plotted vs. pH in Figure 1. The dependence of the rate on pH is exceedingly complex, as several breaks in the curve are apparent for all of the Schiff bases. The relationship between the observed rate constant (k_{obsd}) and the buffer concentration is also quite complex. At relatively high pH (above 5–7, depending on the identity of the imine), plots of k_{obsd} vs. the total buffer concentration ($[B]_t$) are linear. However, at lower pHs there is pronounced curvature for all compounds (Figure 2).

A complete analysis of these results may be obtained by using the generally accepted mechanism for Schiff base hydrolysis, as recently modified by Sayer et al.[20] Schiff base hydrolysis is known to proceed through the intermediate formation of a carbinolamine which subsequently breaks down to products (eq 1). Several investigations have established that

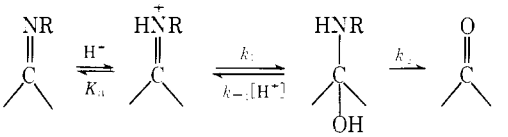

(1)

formation of the carbinolamine (k_1) is usually rate determining at high pH and breakdown to products rate determining at lower pHs.[21-25]

Above pH 5–7, depending on the Schiff base, the rate constants for **2a–g** are satisfactorily accounted for by assuming rate-determining formation of carbinolamine so that k_{obsd} is given by

$$k_{obsd} = k_1[H^+]/([H^+] + K_a) \quad (2)$$

$$= (k_1^{H_2O} + k_1^{OH^-}[OH^-] + k_1^{cat}[B])\left(\frac{[H^+]}{[H^+] + K_a}\right) \quad (2a)$$

where $k_1^{H_2O}$, $k_1^{OH^-}$, and k_1^{cat} are the rate constants for water attack, hydroxide ion attack, and general-base-catalyzed water attack on the protonated Schiff base ($2H^+$). Calculated values of these parameters are given in Table I.

As the pH is lowered below 5–7, a sharp break occurs in the pH–rate profiles of most of the Schiff bases. This break is ascribed to the usual transition from rate-determining attack of water at moderate pH to breakdown of the carbinolamine at low pH. As expected from previous studies[11] of Schiff base hydrolysis, k_{obsd}^0 decreases with increasing $[H^+]$ for most of the pH–rate profiles shown in Figure 1. However, at still lower pH, another break occurs in the pH–rate profiles of **2b, 2d, 2e,** and **2g.** While breaks in the profiles of **2e** and **2g** may be expected due to the protonation of the carboxylate groups at low pH, the breaks observed for **2b** and **2d** must be due to another change in rate-determining step below pH 3. The effect of increasing buffer concentration on k_{obsd} at low pH is also suggestive of another change in rate-determining step. In contrast to the linear buffer plots obtained at high pH, plots of k_{obsd} vs. total buffer concentration ($[B]_t$) at low pH are decidedly nonlinear, as illustrated for the hydrolysis of **2b** at pH 3.45 (Figure 2). Attempts to correlate these results with the steady-state equation for a simple two-step mechanism (eq 3)

$$k_{obsd} = \frac{k_1K_1k_2}{k_1[H^+] + K_1k_2}\left(\frac{[H^+]}{[H^+] + K_a}\right) \quad (3)$$

$$K_1 = k_1/k_{-1}$$

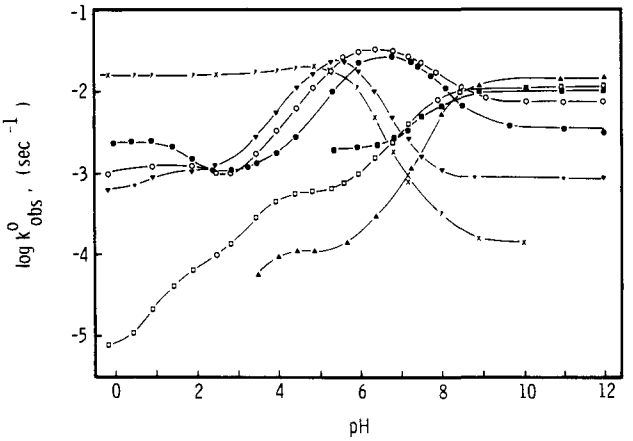

Figure 1. pH–rate profiles for the hydrolysis of **2a** (▲), **2b** (□), **2c** (x), **2d** (▼), **2e** (○), **2f** (■), and **2g** (●), extrapolated to zero buffer concentration at 25 °C and ionic strength 1.0 (NaCl). The complete profiles for **2a–d** and **2f** are theoretical curves calculated from eq 2, 3, and 4 and the kinetic parameters in Tables I and II. The curves for **2e** and **2g** are theoretical only above pH 7.

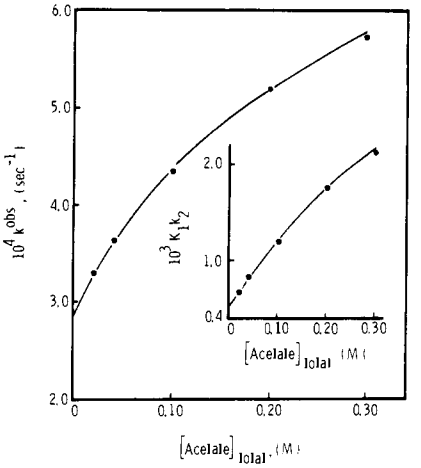

Figure 2. The variation of the observed rate constant (k_{obsd}) for hydrolysis of **2b** with the concentration of acetate buffer, 90% acid, at pH 3.45. The inset shows the dependence of the rate constant for rate-limiting carbinolamine breakdown, K_1k_2, on buffer concentration under the same conditions. The lines are theoretical curves based on the parameters for **2b** in Tables I and II and eq 2, 3, and 4a.

were unsuccessful, and it became apparent that the breakdown of the carbinolamine itself undergoes a change in rate-determining step as the buffer concentration is increased. For example, when values of K_1k_2 were determined from eq 3 as described in the Experimental Section and plotted vs. the total buffer concentration at constant pH, these plots were decidedly nonlinear (Figure 2, inset). Since K_1 is a constant, the variation of k_2 with buffer concentration must be nonlinear. Consequently, there must be a change in rate-determining step for carbinolamine decomposition (k_2) with increasing buffer concentration.

Fortunately, there is precedent for this situation in the elegant work of Sayer et al.[20] They found that several different pathways are available for carbinolamine breakdown to free amine plus the aldehyde or ketone (Scheme I). This intermediate may decompose through either a positively charged species (T^+) or a zwitterion ($T^\pm$). Furthermore, these species are interconvertible through a complex series of reactions. Using this mechanism, the rate constants for several different processes were determined by an examination of the variation of $K_1k_2^0$ (the value of K_1k_2 extrapolated to zero buffer concentration) with pH. Values of $K_1k_2^0$ were calculated as described in the Experimental Section.

Scheme I

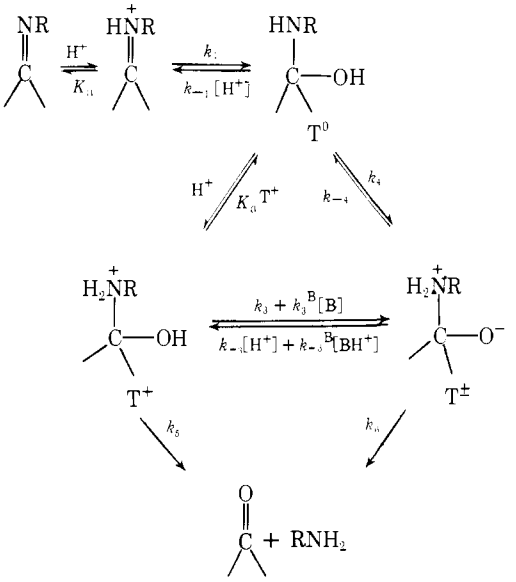

Table II. Rate Constants for Carbinolamine Breakdown in the Hydrolysis of **2**[a]

	Schiff base			
	2a	**2b**	**2c**	**2d**
$10^7 K_1k_4$, M^{-1} s^{-1}	>1.0	1.6	9.0	6.5
$10^6 K_1K_4k_6$, M^{-1} s^{-1}		2.0		30
$10^4 K_1k_3/K_a^{T^+}$, s^{-1}		1.0		5.5
$10^4 K_1k_5/K_a^{T^+}$, s^{-1}		0.069	170	6.5
k_3^B, M^{-1} s^{-1}				
$ClCH_2COO^-$		0.0021		0.03
CH_3COO^-		0.10		1.0

[a] At 25.0 °C with ionic strength = 1.0 (NaCl); parameters, as defined in Scheme II, were determined using eq 4 as described in the Experimental Section.

Application of the steady-state assumption to T^0, T^+, and $T^\pm$ of Scheme I gives an expression for $K_1k_2^0$ as a function of $[H^+]$

$$K_1k_2^0 = K_1\left[\frac{k_5[H^+]}{K_a^{T^+}} + \frac{k_6K_4(k_3[H^+]/K_a^{T^+} + k_4)}{k_6K_4 + k_3[H^+]/K_a^{T^+} + k_4}\right] \quad (4)$$

where $K_4 = k_4/k_{-4}$. The values of $K_1k_2^0$ for **2b** and **2d** were fit to eq 4 as described in the Experimental Section and the parameters obtained are summarized in Table II. It must be emphasized that all four parameters are required in order to obtain the excellent fit with the pH–rate profiles (Figure 1) for **2b** and **2d**.

The rate of carbinolamine breakdown for the Schiff base from trifluoroethylamine (**2c**) showed a simpler kinetic behavior. The value $K_1k_2^0$ was found to be linear with hydrogen ion concentration. This result can be readily accounted for if the term in $k_3[H^+]/K_a^{T^+}$ makes no contribution to the kinetics, i.e., there is no direct interconversion between T^+ and $T^\pm$. Equation 4 then reduces to

$$K_1k_2^0 = K_1\left[\frac{k_5[H^+]}{K_a^{T^+}} + \frac{k_6K_4k_4}{k_6K_4 + k_4}\right] \quad (5)$$

A plot of $K_1k_2^0$ vs. $[H^+]$ gave values for $K_1k_5/K_a^{T^+}$ (slope) and $K_1k_6K_4k_4/(k_6K_4 + k_4)$ (intercept). A comparison of the relative values of k_4 and K_4k_6 as a function of amine pK_a for **2b** and **2d** suggests that $K_4k_6 \gg k_4$ for **2c**. Consequently the in-

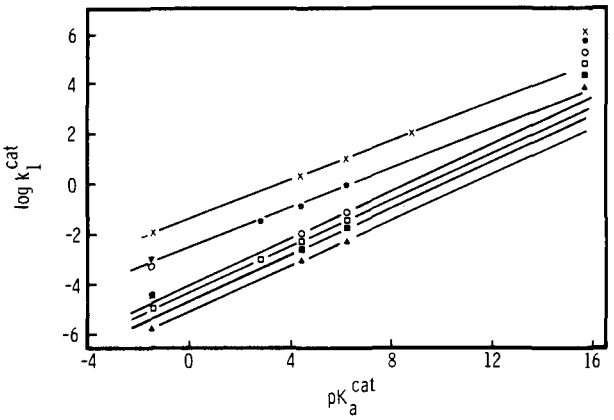

Figure 3. Brønsted plots of the catalytic constants, $k_1^{cat.}$, for the general-base-catalyzed hydrolysis of **2a** (▲), **2b** (□), **2c** (x), **2d** (▼), **2e** (○), and **2f** (■). Values of k_1^{cat} are from Table I; the $pK_a^{cat.}$ values were obtained from pH measurements made under the experimental conditions (25 °C and ionic strength 1.0 with NaCl).

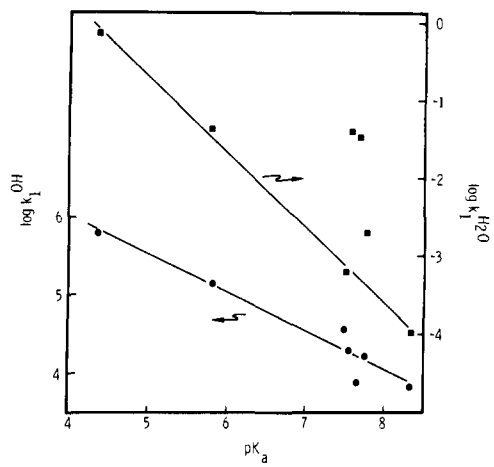

Figure 4. Correlations of the rate constants for water attack, $k_1^{H_2O}$ (■, slope −0.98), and hydroxide ion attack, $k_1^{OH^-}$ (●, slope −0.49) with Schiff base pK_a for the hydrolysis of **2a–g**.

tercept reduces to K_1k_4. These assignments of the two rate constants for **2c** are consistent with the work of Sayer et al.[20] on carbinolamine formation. Their results show that as a Schiff base becomes less basic, the ratios k_3/k_5 and k_{-4}/k_6 continue to decrease until the only significant routes for carbinolamine breakdown become zwitterion formation from T^0 (k_4) at moderate pH and breakdown of T^+ to products (k_5) at low pH. Thus, only one change in rate-determining step is observed for a weakly basic amine corresponding to the usual transition from breakdown of the carbinolamine intermediate to its formation.

A similar detailed analysis of the rate constants for carbinolamine breakdown could not be carried out for **2e, 2f,** and **2g** owing to the complicating ionization of the carboxyl groups. For **2a** only a minimum value for K_1k_4 could be obtained. All rate constants for carbinolamine breakdown are given in Table II.

Discussion

Rate-Determining Nucleophilic Attack. At sufficiently high pH (>5–7), the pH–rate profiles for all of the compounds in this study are satisfactorily explained by rate-limiting attack of water or hydroxide ion on the protonated Schiff base, similar to previous studies of Schiff base hydrolysis.[11,18,21-25] As expected,[11,18,25] the attack of water is general base catalyzed by a wide variety of bases (Table I). A Brønsted plot of the catalytic constants for general base catalysis ($k_1^{cat.}$) vs. the pK_a of the general base gives a straight line for all Schiff bases, with slopes varying from 0.36 to 0.45 (Figure 3). These values are comparable to the Bronsted coefficients of 0.27 and 0.4 previously observed for general-base-catalyzed attack of water on the cationic Schiff bases benzhydrylidenedimethylammonium ion[25] and 2,2,2-trifluoro-*N*-(3-methyl-2-cyclohexenylidene)ethylammonium ion,[18] respectively. For all compounds studied, the rate constant due to hydroxide ion ($k_1^{OH^-}$) shows a large positive deviation (ca. 10^2-fold) in the Bronsted plots. This deviation presumably arises from hydroxide ion acting as a nucleophile rather than a general base catalyst for water attack, similar to what has been observed for other Schiff bases.[11,23,25]

The existence of intermolecular general base catalysis of water attack on $2H^+$ suggests that the internal carboxylate ions in **2e–g** may be capable of acting as intramolecular catalysts. Evidence that this occurs may be found in Figure 3. Although the second-order rate constants for attack of water ($k_1^{H_2O}$/55 M) fall on the Brønsted plot for those Schiff bases without internal carboxylate ions (**2a–d**), this rate constant shows a positive deviation for the Schiff bases from both glycine (**2e**) and alanine (**2f**). The Brønsted plot for **2e** exhibits a value of $k_1^{H_2O}$ which is ca. 30-fold larger than that predicted, whereas $k_1^{H_2O}$ for **2f** is about fivefold greater than expected. These enhanced rates for water attack on $2eH^+$ and $2fH^+$ are consistent with internal general base catalysis by the carboxylate ions.

Another indication of the increased reactivities of the protonated forms of **2e** and **2f** is found in a plot of $k_1^{H_2O}$ vs. the pK_a of the Schiff base (Figure 4). Those compounds without an internal carboxylate ion (**2a–d**) generate a straight line of slope −0.98, similar to what was observed in the hydrolysis of Schiff bases from substituted benzaldehydes, and consistent with a late transition state.[23] The rate constants for water attack for **2e** and **2g,** however, show positive deviations of 60-fold from this correlation, while the corresponding rate constant for **2f** shows a more modest enhancement of about fivefold. The positive deviations for **2e–g** in both the above plots clearly show an enhanced reactivity for their cations toward attack of water. The most reasonable mechanism to account for this result is internal general base catalysis by the carboxylate ions (**3**).

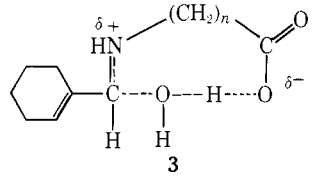

3

In contrast to the plot of log $k_1^{H_2O}$ vs. pK_a, a plot of log $k_1^{OH^-}$ vs. pK_a shows no significant deviations for the rate constants for **2e–g** from the line defined by **2a–d** (Figure 4).[26] Similarly, plots of log $k_1^{cat.}$ vs. pK_a for both acetate- and phosphate-catalyzed rates (not shown) have slopes of −0.82 and −0.78, respectively, and reveal only minor rate enhancements (less than twofold) for **2e–g.** The lack of any increased rates of these processes for Schiff bases containing carboxyl groups is consistent with internal general base catalysis. Such catalysis would only be expected for attack of water and would not be superimposed on external general base catalysis or nucleophilic attack by hydroxide ion.

The enhancements of $k_1^{H_2O}$ for **2e** and **2f** observed in the Brønsted plots may be used to estimate the effective concentration of the carboxylate group arising from its forced proximity to the reactive site. The pK_a of the carboxyl group in **2e** should be comparable to the carboxyl pK_a of glycine (2.35), and from the Brønsted plot for **2e,** a general base of this pK_a should have an *inter*molecular catalytic constant of ca. 1.2×10^{-3} M^{-1} s^{-1}. By correcting the value of $k_1^{H_2O}$ for the small

amount of water attack predicted by the Brønsted plot and dividing by the projected rate for the intermolecular process, an estimate of ca. 30 M is obtained for the effective concentration of the internal base in **2e**. An analogous calculation for **2f** gives an effective concentration of ca. 1 M for the carboxylate group in this Schiff base.

Owing to the presence of two internal general bases in **2g**, the individual catalytic effects of each group are difficult to determine. However, if the carboxyl groups in **2g** function with approximately the same catalytic ability as the corresponding bases in **2e** and **2f**, and if the slope of the Brønsted plot for **2g** is approximately the same as determined for **2b** ($\beta \approx 0.44$), then the intramolecular rate constant for **2g** would be predicted to be ca. 3×10^{-2} s^{-1}. This estimate is in good agreement with the measured value of 3.2×10^{-2} s^{-1} and shows that the enhancement in the rate of hydrolysis of **2g** is also probably due to intramolecular general base catalysis.

Although intramolecular general base catalysis of water attack is in accord with all the data, an alternate explanation for the increased reactivities of **2e–g** toward water attack must be considered. This would involve nucleophilic participation by the carboxylate anion, generating an uncharged cyclic compound, such as **4**, which could protonate to give **4**H$^+$ (Scheme II). Attack of water or hydroxide ion on either species

Scheme II

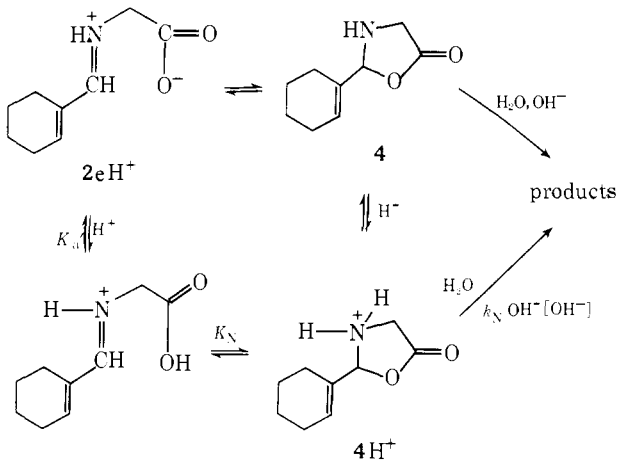

could presumably lead to products.[27] Any significant contribution by such a nucleophilic mechanism to the rate of hydrolysis is considered unlikely for several reasons.

First, on the basis of the absorbance spectra of **2e**, the equilibrium concentrations of the cyclized species, **4** and **4**H$^+$, must be quite small. The extinction coefficient of **2e** at 260 nm is constant from pH 1 to pH 5 (1.9×10^4) and compares well to the extinction coefficients of the other protonated Schiff bases (ca. 2×10^4). In addition, the K_a value of **2e**H$^+$ was determined in solutions ranging in pH from 1 to 12 and no anomalies were observed. The absorbance change at 260 nm should be a more complex function of [H$^+$] if any significant fraction of the Schiff base was converted to **4**, owing to the possible protonation of **4** to form **4**H$^+$. Indeed, the pK_a of **2e**H$^+$ is comparable to the pK_a of **2b**, a Schiff base derived from an amine similar in basicity to glycine.

The kinetic behavior of **2e** is also entirely consistent with the hydrolysis of the protonated Schiff base, and the K_a value determined from a kinetic analysis agrees with that obtained spectrally. Although attack of water and hydroxide ion on **4** (in rapid equilibrium with **2e**H$^+$) would also be consistent with the rate law (eq 2), the good correlation of $k_1^{OH^-}$ for **2e** with the rate constants for the other Schiff bases (Figure 4) argues that hydroxide ion attack on **4** is not significant, and the uncatalyzed attack of water for the hydrolysis of an ester such as **4** would be much too slow to account for $k_1^{H_2O}$ (0.037 s^{-1}). Water attack on **4**H$^+$ is inconsistent with the observed rate law,[28] leaving hydroxide ion attack on **4**H$^+$ as the only viable alternative to explain the kinetic behavior of **2e**. By this mechanism, the pH-independent rate at pH 6–7 for **2e** ($k_1^{H_2O}$) would actually be represented by $k_1^{H_2O} = K_N k_N^{OH^-} K_w / K_a'$. Substituting values of $k_1^{H_2O}$ (0.037 s^{-1}), K_w (10^{-14}), and K_a' (ca. 5×10^{-3}, analogous to glycine) into this expression yields $K_N k_N^{OH^-} \approx 2 \times 10^{10}$ M^{-1} s^{-1}. On the basis of the large extinction coefficient observed for **2e** at pH 1, it is obvious that K_N is much less than 1, and this leads to a value for $k_N^{OH^-}$ which exceeds the rate of diffusion. Therefore, species **4** and **4**H$^+$ cannot be kinetically significant in the hydrolysis of **2e**.

By an analysis similar to that outlined above for **2e**, nucleophilic participation by the carboxylate groups in the hydrolysis of **2f** and **2g** is also considered improbable. The good correlation of $k_1^{OH^-}$ for **2f** and **2g** with the rate constants for other Schiff bases (Figure 4), the reasonable pK_a's, the large extinction coefficients in acidic solution, and the observed rate law all are consistent with the reactive species being the protonated Schiff base. The minimum value of $k_N^{OH^-}$ estimated for **2f**, in an attempt to account for $k_1^{H_2O}$ by hydroxide ion attack on a protonated cyclic species analogous to **4**H$^+$, is ca. 5×10^8 M^{-1} s^{-1}.[29] Although this rate does not exceed the diffusion rate as it did for **2e**, it seems unlikely for nucleophilic attack on an acyl carbon. Since nucleophilic catalysis apparently does not operate in the hydrolysis of **2e** or **2f**, it is reasonable to expect that such a mechanism does not occur in the hydrolytic reaction of **2g** either.

Other examples of internal catalysis of Schiff base formation or hydrolysis are rare. Intramolecular general base catalysis by an ionized *o*-OH group was originally suggested for the hydrolysis of Schiff bases derived from salicylaldehyde[30] and from 3-hydroxypyridine-4-carboxaldehyde.[31] However, subsequent investigation of the hydrolysis of *o*-, *m*-, and *p*-hydroxy-*N*-benzylidene-2-aminopropane and their methoxy analogues indicate that internal catalysis by $-O^-$ in the ortho position does not occur.[32] Hine et al.[33] presented evidence for internal acid-catalyzed dehydration of carbinolamines formed from acetone and various substituted amines. In addition, Sayer et al.[20b] concluded that substituted hydrazines with a moderately acidic proton may provide intramolecular general acid catalysis in the formation of carbinolamines from carbonyl compounds and amines.

The larger effective concentration of the intramolecular base in **2e** (30 M) compared to **2f** (1 M) suggests that the insertion of an additional methylene group between the imine linkage and the internal base in **2f** significantly decreases the efficiency of intramolecular catalysis. A similar effect was noted in the internal-acid-catalyzed dehydration of carbinolamines derived from monoprotonated diamines of the structure HN$^+$-(Me)$_2$(CH$_2$)$_n$NH$_2$.[33] Thus, as n was increased from 2 to 3 or 4, the rate of Schiff base formation decreased by ca. tenfold, although the increased basicity of the primary amine groups would be expected to increase the rate in the absence of internal catalysis. Therefore, the more efficient internal catalysis observed for 1,2-diamines closely parallels the 30-fold difference measured for **2e** and **2f**.

Rate-Limiting Breakdown of the Carbinolamine Intermediate. As noted in the Results, the rate constants for breakdown of the carbinolamine intermediate do not vary with pH as expected for the simple two-step mechanism for Schiff base hydrolysis.[11] The pH–rate profile for **2b** clearly indicates another break below pH 3. The initial decrease in the rate of hydrolysis of **2b** that occurs below pH 4 is no doubt due to the transition from rate-determining nucleophilic attack on **2b**H$^+$ to decomposition of an intermediate. Usually, the rate of Schiff base hydrolysis decreases linearly with respect to hydroxide ion

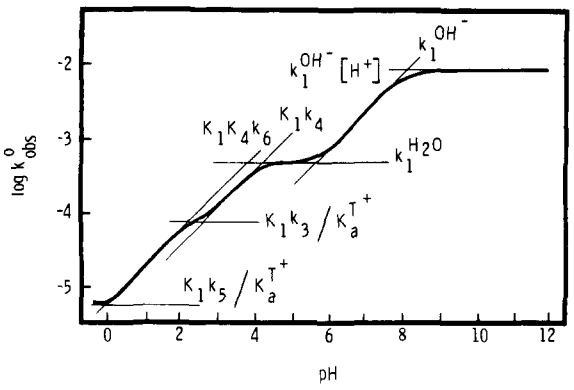

Figure 5. pH–rate profile for the hydrolysis of **2b**, illustrating the various changes in rate-determining step.

concentration at low pH.[11,23,25] This has been ascribed to the concentration of the zwitterion intermediate ($T^{\pm}$) decreasing

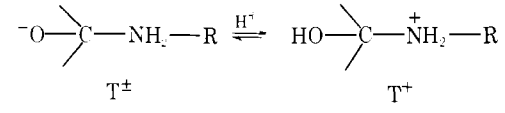

$T^{\pm}$ T^{+}

in direct proportion to pH, which results in the formation of the unreactive (or, at least, less reactive) protonated carbinolamine (T^{+}).[11] The rate of hydrolysis of **2b**, however, levels off near pH 2.5, only to decrease further and level off again as the pH is lowered (Figure 1).

Unusually high rates of hydrolysis at low pH have been reported for some aromatic Schiff bases,[23,25] but these anomalies had gone unexplained until the recent elegant work by Sayer et al.[20] These authors have shown that carbinolamine formation can occur by two separate mechanisms: (1) acid-catalyzed amine attack in a "more or less concerted" manner, and (2) a stepwise process involving uncatalyzed formation of a zwitterion that is subsequently trapped by proton transfer from water or acids. Accordingly, the reverse process, Schiff base hydrolysis, can occur as outlined in Scheme I.

Using this mechanism, the pH–rate profile for the hydrolysis of a typical Schiff base (**2b**) may be rationalized in the following way (Figure 5). At high pH (>4), the rate-determining step is carbinolamine formation (k_1); between pH 4 and 6 attack takes place by water on the protonated Schiff base ($k_1^{H_2O}$), whereas above pH 6 hydroxide ion is the nucleophile ($k_1^{OH^-}$). The break at ca. pH 8 is due to ionization of the Schiff base. As the pH is lowered below 4, a rapid prior equilibrium exists between the protonated Schiff base and the carbinolamine, and the rate-determining step becomes the proton-switch[20a] process (k_4) which interconverts T^0 and $T^{\pm}$. Slightly below pH 3, the stepwise pathway for conversion of T^0 to $T^{\pm}$ ($k_3/K_a^{T^+}$) becomes competitive with k_4 and the pH–rate profile levels off. At still lower pHs (<2), k_{-3} [H^+] is greater than k_6, and k_6 becomes rate limiting. At higher acidity (pH $(H_0) \leq 0$), the neutral transition state from $T^{\pm}$ becomes less stable than the positively charged one from T^+ and the reaction proceeds through rate-limiting breakdown of T^+ (k_5).

Values for the microscopic rate and equilibrium constants of Scheme I were obtained by using the procedure of Sayer and Jencks[20c] to calculate $pK_a^{T^+}$ and K_3, and by noting that k_{-3} should be diffusion controlled ($\sim 10^{10}$ M^{-1} s^{-1}). The calculated values are given in Table III. Consistent with the observation of this type of multistep mechanism, the rate of breakdown of $T^{\pm}$ to products (k_6) is faster than the equilibration of T^0 and $T^{\pm}$ through a "proton switch" mechanism (k_{-4}). The values of k_{-4} for **2b** and **2d** (ca. 10^7 s^{-1}) are in the range previously observed for this process (10^6–10^8 s^{-1}).[34] The rate constants for breakdown of $T^{\pm}$ (k_6) are also comparable to the rate constants for other systems in which multistep reaction pathways of this type can be inferred. The analogous rate constant for amine expulsion from the intermediate $T^{\pm}$ from *p*-chlorobenzaldehyde and methoxyamine[20a] is 5.3×10^8 s^{-1}; for the intermediate from *p*-chlorobenzaldehyde and semicarbazide,[35] it is 2×10^9 s^{-1}. It should be noted, however, that these intermediates are both derived from relatively weakly basic amines (pK_a = 4.70 and 3.86, respectively). It is expected[34,35] that the k_6 term should decrease with increasing amine basicity, however, so that zwitterionic tetrahedral intermediates having more basic amine moieties should decompose substantially slower. For example, the rate constant for breakdown of $T^{\pm}$ from methylamine (pK_a = 10.6) and isobutyraldehyde is about 4.9×10^6 s^{-1}.[13] It is initially surprising then that the k_6 values for **2b** and **2d** are similar to those for zwitterions derived from weakly basic amines and about 100-fold faster than the rate constant from the zwitterion of isobutyraldehyde and methylamine. Indeed, to our knowledge, these changes in rate-determining steps have not previously been observed with amines as basic as ethanolamine and glycinamide, presumably due to k_6 being less than k_4 in these cases.

Table III. Calculated Values of Rate and Equilibrium Constants for the Processes of Scheme I

	2b	**2c**	**2d**
$pK_a^{T^+}$	7.9	3.6	6.1
K_1, M^{-1}	2.5×10^{-13}		5.3×10^{-11}
K_3, M^{-1}	4.4×10^{-10}	2.4×10^{-9}	7.6×10^{-10}
K_4, M^{-1}	4.1×10^{-2}	9.6×10^{-6}	1.0×10^{-3}
k_3, s^{-1}	4.4	24	7.6
k_{-3}, M^{-1} s^{-1}	10^{10}	10^{10}	10^{10}
k_4, s^{-1}	6.5×10^5		1.2×10^4
k_{-4}, s^{-1}	1.6×10^7		1.2×10^7
k_5, s^{-1}	0.30		9.0
k_6, s^{-1}	2.0×10^8		5.5×10^8

The most reasonable explanation for the accelerated breakdown of $T^{\pm}$ from **2b** and **2d** is an enhanced stability of cyclohexene-1-carboxaldehyde (**1**) relative to the other aldehydes. The existence of α,β unsaturation no doubt provides an extra driving force for elimination of amine over that available with *p*-nitrobenzaldehyde or isobutyraldehyde. Support for this hypothesis may be found in the fact that both *p*-nitrobenzaldehyde and isobutyraldehyde are significantly hydrated in aqueous solution (20 and 38%, respectively),[36,37] whereas cyclohexene-1-carboxaldehyde shows no detectable formation of hydrate.[38] These results suggest that elimination of a nucleophile (e.g., amine) from a tetrahedral intermediate should be more favorable when **1** is produced rather than *p*-nitrobenzaldehyde or isobutyraldehyde. Consequently, complex kinetics, characteristic of several changes in rate-determining steps, are observable for more basic amines with **1** than with *p*-nitrobenzaldehyde (or other aldehydes).

Although microscopic rate constants could only be determined for three of the Schiff bases, it is informative to consider the trends in these parameters as the amine pK_a is varied (Table III). It is noteworthy that the dependence of k_5 on Schiff base basicity for **2b** and **2d** ($\Delta \log k_5 = -0.9\Delta pK_a$) is substantially greater than the dependence of k_6 ($\Delta \log k_6 = -0.3\Delta pK_a$). This result suggests that the transition state for the breakdown from T^+ (k_5) is much further along the reaction coordinate than the one for breakdown from $T^{\pm}$ (k_6). In their study of Schiff base formation, Sayer and Jencks[20a] found that variation in the aldehyde portion also had more effect on the rate of breakdown to aldehyde plus amine from T^+ than from $T^{\pm}$.

The general-base-catalyzed breakdown of the carbinolamine intermediate observed at moderate pH is due to catalysis of the proton transfer from the protonated carbinolamine to give the

zwitterion (k_3). If a simple proton transfer is rate determining for the general-base-catalyzed process, the Brønsted slope should be near zero when the proton transfer is thermodynamically favored (at high pK_a for the base catalyst), and approch 1.0 as the base catalyst decreases in pK_a.[40] Strong bases could not be used in the low pH region to confirm the expected curvature in the Brønsted plot but the estimated β from the k_3^B values for **2b** is near 1.0 and supports the rate-determining transfer of a proton.

Although general base catalysis by external buffers of carbinolamine breakdown was clearly observable for **2**, it was not possible to unambiguously determine whether intramolecular general base catalysis of this process exists. The inability to determine all the kinetic parameters for more than two Schiff bases precludes a comparison of these rate constants in both the presence and absence of a carboxylate ion. The pH-rate profiles of **2e** and **2g** are further complicated by the ionization of the internal bases in these two compounds. The increases observed in k_{obsd}^0 for **2e** and **2g** as the pH is lowered below 2.5 (Figure 1) may be attributed to protonation of the carboxylate groups. Neutralizing the carboxylate anion decreases the nitrogen basicities of **2e** and **2g** which then leads to increases in the rates of carbinolamine breakdown. The plateau from pH 0 to 2 in the profile of **2e** is similar to that observed for **2d** and probably reflects the decrease in the iminium pK_a of **2e**H$^+$ by ~2 pK_a units. This pK_a decrease is analogous to that observed when the carboxylate group of glycine is replaced by an amide or ester function.

Experimental Section

Materials. Distilled water was used for all kinetic solutions. Buffers were reagent grade and used without purification. Ethanolamine and *n*-propylamine were purified by distillation, as was 2,2,2-trifluoroethylamine after neutralization of its hydrochloride salt. Glycinamide was obtained from its hydrochloride salt by neutralization with sodium hydroxide in methanol followed by removal of the solvent. The crude glycinamide was repeatedly dissolved in absolute ethanol, cooled, and filtered until 95% of the theoretical amount of sodium chloride was separated; recrystallization from absolute ether yielded the pure amide. Glycine, β-alanine, and aspartic acid were reagent grade and used without purification. Cyclohexene-1-carboxaldehyde (**1**) was prepared according to the procedure of Braude and Evans,[41] bp 61–63 °C (11 mm) (lit.[41] bp 72 °C (15 mm)). The Schiff bases (**2a–g**) were prepared from **1** as described below.

Preparation of Schiff Bases of Cyclohexene-1-carboxaldehyde. Schiff bases **2a–c** were prepared by mixing the amine (5 mmol) with **1** (5 mmol) in 5 mL of absolute ether over molecular sieves at room temperature. After 1–2 h, analysis by IR revealed that no aldehyde remained; decanting from the sieves and removal of the solvent gave quantitative yields of the Schiff bases. Schiff base **2d** was obtained by an analogous procedure using absolute ethanol as the solvent. Compounds **2e–g** were prepared by reacting the potassium or sodium salt of the amino acid (17 mmol) with **1** (17 mmol) in 10 mL of absolute methanol for 30 min under nitrogen, analogous to the procedure given by Heinert and Martell.[42] The solvent was removed, the gummy residue treated with dry acetonitrile and evaporated to dryness under vacuum, and the residue treated with absolute ether to yield crystals. Purification procedures, spectra, and elemental analyses are given below. The salts **2e–g** (recrystallized) were sealed in capillary tubes and were used to prepare fresh stock solutions in absolute methanol shortly before use. Stock solutions of purified **2a–d** were prepared in dry acetonitrile and were stable indefinitely when stored under refrigeration.

2a. Analytic and kinetic samples were obtained by GLC (Silicone DC-55): IR (Et_2O) 1642 and 1629 cm^{-1} (C=N and C=C); NMR (CCl_4) δ 7.38 (s, 1, CH=N), 5.75 (m, 1, C=CH), 3.20 (t, J = 7 Hz, 2, C=NCH$_2$), 2.38–1.8 (m, 4), 1.85–1.30 (m, 6), 0.86 (t, J = 7 Hz, 3); UV (H_2O, pH 2) λ_{max} 259 nm (ϵ 1.87 × 10^4).

Anal. Calcd for $C_{10}H_{17}N$: C, 79.41; H, 11.33; N, 9.26. Found: C, 79.26; H, 11.28; N, 9.11.

2b. Purification by vacuum distillation; bp 80 °C (0.05 mm); IR (Et_2O) 1644 and 1629 cm^{-1} (C=N and C=C); NMR ($CDCl_3$) δ 7.78 (s, 1), 6.15 (s, 1), 3.9–3.4 (m, 5), 2.4–1.9 (m, 4), 1.9–1.4 (m, 4); UV (H_2O, pH 2) λ_{max} 262 nm (ϵ 1.94 × 10^4).

Anal. Calcd for $C_9H_{15}NO$: C, 70.56; H, 9.87; N, 9.14. Found: C, 70.42; H, 9.80; N, 9.38.

2c. Purification by GLC (5% Carbowax); IR (Et_2O) 1643 and 1629 cm^{-1} (C=N and C=C); NMR (CCl_4) δ 7.45 (s, 1), 5.93 (m, 1), 3.71 (q, J = 9 Hz, 2, CH_2CF_3), 2.4–1.9 (m, 4), 1.9–1.4 (m, 4); UV (H_2O, pH 2) λ_{max} 260 nm (ϵ 2 × 10^4).

Anal. Calcd for $C_9H_{12}NF_3$: C, 56.54; H, 6.32; N, 7.33. Found: C, 56.45; H, 6.40; N, 7.35.

2d. The crude crystals were extracted with dry ether and the solution concentrated with cooling to promote crystallization. A white powder was isolated in 60% yield. Analysis by NMR revealed the presence of <5% glycinamide. Attempts to purify the powder further by recrystallization only resulted in discoloration and a lowered melting point. The elemental analysis given below shows a slightly low carbon content which can be explained by the presence of 3–4% glycinamide. Small amounts of glycinamide were shown to have no effect on the kinetic behavior of **2d** in dilute solutions: mp 81–84 °C; IR ($CHCl_3$, 4%) 3510, 3450, 1680 ($CONH_2$), 1642 and 1628 cm^{-1} (C=N and C=C); NMR ($CDCl_3$) δ 7.52 (s, 1), ca. 6.5 (broad s, 2, $CONH_2$), 6.01 (m, 1), 3.92 (s, 2), 2.5–1.9 (m, 4), 1.9–1.4 (m, 4); UV (H_2O, pH 2) λ_{max} 264 nm (ϵ 1.9 × 10^4).

Anal. Calcd for $C_9H_{14}N_2O$: C, 65.03; H, 8.44; N, 16.86. Found: C, 63.60; H, 8.42; N, 17.10.

2e. Recrystallization twice from ethanol–ether (1:5) gave white needles in a 70% yield. Elemental and IR analyses revealed that **2e** exists as a monohydrate; this is not unusual for potassium salts of amino acid derived Schiff bases.[35] Ir (KBr) 1590 (broad), 1400, 750 (COO^-K^+), 1640 and 1625 cm^{-1} (C=N and C=C); NMR (MeOH) δ 7.40 (s, 1), 5.98 (s, 1) 3.83 (s, 2); UV (H_2O, pH 1–4) λ_{max} 261 nm (ϵ 1.9 × 10^4).

Anal. Calcd for $C_9H_{12}NO_2K\cdot H_2O$: C, 48.41; H, 6.32; N, 6.27. Found: C, 48.44; H, 6.07; N, 6.40.

2f. Recrystallization from acetonitrile–methanol (5:1) yielded hygroscopic crystals: IR (KBr) 1585 (broad), 1395, 748 (COO^-K^+), 1640 and 1624 cm^{-1} (C=N and C=C); NMR (MeOH) δ 7.50 (s, 1) and 6.02 (s, 1); UV (H_2O, pH 1–5) λ_{max} 262 nm (ϵ 1.75 × 10^4).

Anal. Calcd for $C_{10}H_{14}NO_2K$: C, 54.76; H, 6.43; N, 6.39. Found: C, 54.35; H, 6.75; N, 6.30.

2g. Recrystallized from methanol–ether; IR (KBr) 1585 (broad) and 1410 (COO^-), 1640 cm^{-1} (shoulder, C=N or C=C); UV (H_2O, pH 1) λ_{max} 264 nm (ϵ 1.80 × 10^4).

Anal. Calcd for $C_{11}H_{13}NO_4K_2\cdot 2H_2O$: C, 39.15; H, 5.03; N, 4.14. Found: C, 39.36; H, 5.27; N, 4.05.

Determination of Schiff Bases Ionization Constants. The K_a values for all Schiff bases were determined spectrally. A constant volume of a stock solution of the purified Schiff base was mixed with buffer solutions of varying pH at constant ionic strength (1.0, NaCl) and temperature (25.0 ± 0.2 °C). Initial absorbance readings at 260 nm (A) were obtained by extrapolation to the time of mixing and used to calculate K_a from the equation

$$[H^+] = K_a\left(\frac{A_b - A}{A - A_a}\right)$$

where [H$^+$] was obtained from the measured pH, and A_a and A_b are initial absorbances at 260 nm measured at pH 2 and 12, respectively. A least-squares fit of the above equation was forced through an intercept of zero to give the K_a values listed in Table I.

For some Schiff bases (**2a**, **2b**, and **2e**) K_a values were also determined using a rearranged form of eq 2a in the text:

$$k_{obsd}^0 = k_1^{H_2O} + \frac{(k' - k_{obsd}^0)}{[H^+]}K_a$$

In this equation, k_{obsd}^0 is k_{obsd} extrapolated to zero buffer concentration, and $k' = (10^{-14}k_1^{OH^-})/K_a$, which is the observed pH-independent rate constant obtained at high pH. Least-squares fits of this equation yielded K_a values from the slopes which are also listed in Table I.

Kinetic Methods. All kinetic measurements were carried out at 25.0 ± 0.2 °C and at ionic strength maintained at 1.0 with NaCl. pH measurements were made on a Radiometer Model 26 pH meter. Spectra were obtained on a Cary 16K and rates were followed using either a Gilford 2000 or 2400 spectrophotometer. All observed rate constants were pseudo-first order and were calculated using a nonlinear least-squares analysis. Rates of Schiff base disappearance were

measured at 235 nm when **2** was present primarily as the free base or at 260 nm when the Schiff base was protonated. In some cases, the rates of appearance of **1** at 240 nm were also monitored and the observed rate constants were found to agree with rates measured at 260 nm within 5%.

Except at pH 0–3 and 11–13, where HCl or NaOH was used, buffers were employed to keep pH constant. Rate constants were extrapolated to zero buffer concentration as described below.

(a) In the pH region where attack on protonated **2** is predominantly rate determining (above pH 5–7, depending on the Schiff base), plots of observed rate constants vs. total buffer concentration, $[B]_t$, were linear and were extrapolated to zero buffer concentration using a weighted least-squares analysis. The slopes obtained were first corrected for the fraction of **2** present as the free base (i.e., slope $\times$ $(K_a + [H^+])/[H^+]$) and these corrected slopes were plotted vs. the fraction of the buffer present as the free base to give rate constants for base-catalyzed water attack ($k_1^{cat.}$) listed in Table I. Catalysis by the acid form of the buffer was zero within experimental error in all cases.

(b) Below pH 5–7 plots of k_{obsd} vs. $[B]_t$ were not linear and buffer independent rate constants were obtained by two different procedures. At low pH, where carbinolamine breakdown is largely rate determining, plots of k_{obsd} vs. $[B]_t$ could be extrapolated to zero buffer concentration to yield k_{obsd}^0 directly because curvature of the plots was minimal at low $[B]_t$ in this pH region. Values of $K_1k_2^0$ were calculated from k_{obsd}^0 using eq 3 and values of k_1^0 obtained from results at higher pH. However, at moderate pH plots of k_{obsd} vs. $[B]_t$ showed more pronounced curvature (Figure 2) and direct extrapolation to give k_{obsd}^0 was difficult. In this transitional pH range, where neither formation nor breakdown of the carbinolamine is predominantly rate limiting, plots of K_1k_2 vs. $[B]_t$ were effectively linear at low $[B]_t$ (Figure 2, inset) and were used to obtain $K_1k_2^0$. The plots of K_1k_2 vs. $[B]_t$ were generated using eq 3 from k_{obsd} and values of k_1 calculated from the kinetic parameters obtained for carbinolamine formation at higher pHs (Table I) using eq 2a. Therefore, values of k^0_{obsd} in this transitional pH region were calculated from $K_1k_2^0$ and k_1^0 using eq 3 and were used to construct the pH–rate profile in this pH range (Figure 1).

Analysis of the pH–Rate Data. A. Rate-Determining Nucleophilic Attack. In the region above pH 5–7 the observed rate constants, extrapolated to zero buffer concentration (k_{obsd}^0), were corrected for dissociation of the protonated Schiff base using the measured K_a and then plotted vs. hydroxide concentration according to the equation

$$k^0_{obsd}\left(\frac{[H^+] + K_a}{[H^+]}\right) = k_1^{H_2O} + k_1^{OH^-}[OH^-]$$

which is a rearranged form of eq 2a in the absence of buffer. A least-squares fit of this equation yielded a slope of $k_1^{OH^-}$ and an intercept of $k_1^{H_2O}$. For most Schiff bases this analysis gave values of $k_1^{H_2O}$ quite close to the maximum rate observed at pH 5–7; this arises because the change in rate-determining step to carbinolamine breakdown does not occur, in most cases, until the Schiff base is nearly completely protonated. However, the calculation of $k_1^{H_2O}$ for **2c** required a large extrapolation because nucleophilic attack is predominantly rate limiting only above pH 6.5. Although the pK_a of **2c** is accurately known (4.36 ± 0.02), the large corrections necessary above pH 6.5 magnify any errors in the data. For this reason the $k_1^{H_2O}$ value for **2c** is somewhat uncertain. All calculated values of $k_1^{H_2O}$ and $k_1^{OH^-}$, along with standard deviations, are summarized in Table I.

B. Rate-Determining Breakdown of the Carbinolamine Intermediate. Sufficient data were obtained for the hydrolysis of **2b** to allow the variation of $K_1k_2^0$ with $[H^+]$ to be analyzed in terms of eq 4 of the text as follows.

At high $[H^+]$, $H_0 = -0.21$[43] to pH 1, eq 4 reduces to

$$K_1k_2^0 = K_1\{(k_5[H^+]/K_a^{T^+}) + k_6K_4\}$$

and a plot of $K_1k_2^0$ vs. $[H^+]$ gave $K_1k_5/K_a^{T^+}$ and $K_1k_6K_4$ from the slope and intercept, respectively. At low $[H^+]$ (pH ~ 4), $k_3[H^+]/K_a^{T^+} < k_4$ and the $K_1k_5[H^+]/K_a^{T^+}$ term is negligible; thus, eq 4 reduces in this limiting case to

$$K_1k_2^0 = K_1k_6K_4k_4/(k_6K_4 + k_4)$$

which was used to give a good estimate of the quantity K_1k_4 from the value of $K_1k_6K_4$ determined above. Values for $K_1k_3/K_a^{T^+}$ were then calculated from data in the intermediate pH region 1–4. All the parameters were finally varied slightly to obtain the best fit for the experimental values of $K_1k_2^0$ to eq 4. The constants for **2b** given in Table II describe the entire pH region below pH 4 very well (the root mean square deviation of the experimental points is 1.4%).

Parameters for the breakdown of the intermediate in the hydrolysis of **2d** were also obtained by the procedure outlined above. In this case, however, the values of $K_1k_5/K_a^{T^+}$ and $K_1k_3K_a^{T^+}$ were comparable which resulted in the expression for $K_1k_2^0$ being relatively insensitive to the magnitude of $K_1K_4k_6$, even at low pH. The root mean square deviation of the experimental and calculated points for the parameters (Table II) obtained for **2d** is 3.5% over a pH range of $H_0 = -0.21$ to pH 4.43.

Catalytic rate constants for carbinolamine breakdown (k_3^B) were obtained from plots of K_1k_2 vs. [B] by assuming that the conversion of T^+ to $T^\pm$ is the only process in carbinolamine breakdown which is significantly catalyzed by buffers at moderate pH (Scheme I).[20a] Therefore, in the presence of buffers eq 4 becomes

$$K_1k_2 = K_1\left\{\frac{k_5[H^+]}{K_a^{T^+}} + \frac{k_6K_4[(k_3 + k_3^B[B])[H^+]/K_a^{T^+} + k_4]}{k_6K_4 + (k_3 + k_3^B[B])[H^+]/K_a^{T^+} + k_4}\right\} \quad (4a)$$

Values for k_3^B were varied until plots of K_1k_2 vs. [B] were satisfactorily described by this expression using the other parameters of Table II (see Figure 2).

Acknowledgment. This work was supported by Grant GM 20188 from the National Institutes of Health. We wish to thank Professor W. P. Jencks for his helpful comments.

References and Notes

(1) L. Hellerman and D. S. Coffey, *J. Biol. Chem.*, **242**, 582 (1967).
(2) B. L. Horecker, S. Pontremoli, C. Ricci, and T. Cheng, *Proc. Natl. Acad. Sci. U.S.A.*, **47**, 1942 (1961); E. Grazi, P. T. Rowley, T. Cheng, O. Tchola, and B. L. Horecker, *Biochem. Biophys. Res. Commun.*, **9**, 38 (1962).
(3) E. Grazi, T. Cheng, and B. L. Horecker, *Biochem. Biophys. Res. Commun.*, **7**, 250 (1962); C. Y. Lai, O. Tchola, T. Cheng, and B. L. Horecker, *J. Biol. Chem.*, **240**, 1347 (1965).
(4) R. G. Rosso and E. Adams, *J. Biol. Chem.*, **242**, 5524 (1967).
(5) O. M. Rosen, P. Hoffee, and B. L. Horecker, *J. Biol. Chem.*, **240**, 1517 (1965).
(6) (a) S. Warren, B. Zerner, and F. H. Westheimer, *Biochemistry*, **5**, 817 (1966); (b) F. H. Westheimer, *Proc. Chem. Soc., London*, 253 (1963).
(7) (a) J. R. Butler, W. L. Alworth, and M. J. Nugent, *J. Am. Chem. Soc.*, **96**, 1617 (1974); (b) A. D. N. Vaz, J. R. Butler, and M. J. Nugent, *ibid.*, **97**, 5914 (1975).
(8) R. Jeffcoat, H. Hassall, and S. Dagley, *Biochem. J.*, **115**, 977 (1969).
(9) D. Portsmouth, A. C. Stoolmiller, and R. H. Abeles, *J. Biol. Chem.*, **240**, 2751 (1967).
(10) D. L. Nandi and D. Shemin, *J. Biol. Chem.*, **243**, 1236 (1968).
(11) (a) W. P. Jencks, "Catalysis in Chemistry and Enzymology", McGraw-Hill, New York, N.Y., 1969, pp 490–496; (b) W. P. Jencks, *Prog. Phys. Org. Chem.*, **2**, 63 (1964).
(12) A. Williams and M. L. Bender, *J. Am. Chem. Soc.*, **88**, 2508 (1966).
(13) J. Hine, J. C. Craig, Jr., J. G. Underwood II, and F. A. Via, *J. Am. Chem. Soc.*, **92**, 5194 (1970).
(14) R. M. Pollack and J. D. Copper, *J. Org. Chem.*, **38**, 2689 (1973).
(15) See, for example, the discrepancy (ca. 10^3-fold) between the rates of formation of the Schiff base from acetoacetate decarboxylase and acetoacetic acid compared to the corresponding reaction of acetoacetic acid with the model compound aminoacetonitrile.[16,17]
(16) J. P. Guthrie and F. H. Westheimer, *Fed. Proc., Fed. Am. Soc. Exp. Biol.*, **26**, 562 (1967).
(17) J. P. Guthrie and F. Jordan, *J. Am. Chem. Soc.*, **94**, 9132 (1972).
(18) R. M. Pollack and M. Brault, *J. Am. Chem. Soc.*, **98**, 247 (1976).
(19) (a) R. M. Silverstein and G. C. Bassler, "Spectrophotometric Identification of Organic Compounds", Wiley, New York, N.Y., 1967, p 162; (b) E. M. Kosower and T. S. Sorensen, *J. Org. Chem.*, **28**, 692 (1963).
(20) (a) S. Rosenberg, S. M. Silver, J. M. Sayer, and W. P. Jencks, *J. Am. Chem. Soc.*, **96**, 7986 (1974); (b) J. M. Sayer, B. Pinsky, A. Schonbrunn, and W. Washtien, *ibid.*, **96**, 7998 (1974); (c) J. M. Sayer and W. P. Jencks, *ibid.*, **95**, 5637 (1973).
(21) W. P. Jencks, *J. Am. Chem. Soc.*, **81**, 475 (1959).
(22) R. L. Reeves, *J. Am. Chem. Soc.*, **84**, 3332 (1962).
(23) E. H. Cordes and W. P. Jencks, *J. Am. Chem. Soc.*, **85**, 2843 (1963).
(24) E. H. Cordes and W. P. Jencks, *J. Am. Chem. Soc.*, **84**, 832 (1962).
(25) K. Koehler, W. Sandstrom, and E. H. Cordes, *J. Am. Chem. Soc.*, **86**, 2413 (1964).
(26) The appreciably lower slope for the plot for $k_1^{OH^-}$ (−0.5) compared to the plot for $k_1^{H_2O}$ is consistent with the concept that the transition state for water attack on $2H^+$ is more productlike than the transition state for hydroxide ion attack.[18,23]
(27) M. L. Bender, J. A. Reinstein, M. S. Silver, and R. Mikulak, *J. Am. Chem. Soc.*, **87**, 4545 (1965), report that the hydrolysis of 3-morpholinophthalide may occur by hydroxide ion attack at the acyl carbon, analogous to attack on the hypothetical compound $4H^+$. Such a mechanism left the pH–rate profile below pH 4 unexplained, however, and the involvement of an iminium ion as the reactive species appears more plausible.[11]

(28) Water attack on $4H^+$ would require protonation of **4** to produce $4H^+$, leading to terms in the rate law which would be second order in $[H^+]$. The good fit of the experimental data to eq 1 rules out this possibility.
(29) This value of $K_N^{OH^-}$ for **2f** was estimated using values of $k_1^{H_2O} = 2 \times 10^{-3}$ s^{-1}, $K_a' = 2.5 \times 10^{-4}$ (taken from the value for β-alanine), and $K_N \leq 0.1$ (an upper limit based on the large extinction coefficient measured for $2fH^+$).
(30) R. L. Reeves, *J. Org. Chem.*, **30**, 3129 (1965).
(31) T. C. French, D. S. Auld, and T. C. Bruice, *Biochemistry*, **4**, 77 (1965).
(32) W. Bruyneel, J. J. Charette, and E. DeHoffmann, *J. Am. Chem. Soc.*, **88**, 3808 (1966).
(33) (a) J. Hine, M. S. Cholod, and W. K. Chess Jr., *J. Am. Chem. Soc.*, **95**, 4270 (1973); (b) J. Hine and W. S. Li, *J. Org. Chem.*, **40**, 2622 (1975).
(34) W. P. Jencks and J. M. Sayer, *Faraday Symp. Chem. Soc.*, **10**, 41 (1975).
(35) W. P. Jencks, *Acc. Chem. Res.*, in press.
(36) J. M. Sayer, *J. Org. Chem.*, **40**, 2545 (1975).
(37) (a) J. Hine, J. G. Houston, and J. H. Jensen, *J. Org. Chem.*, **30**, 1184 (1965); (b) L. R. Green and J. Hine, *ibid.*, **38**, 2801 (1973).
(38) By employing the UV method used by Sayer[36] to detect *p*-nitrobenzaldehyde hydration, we were unable to find any hydrated cyclohexene-1-carboxaldehyde.[39]
(39) R. H. Kayser and R. M. Pollack, unpublished observations.
(40) M. Eigen, *Angew. Chem., Int. Ed. Engl.*, **3**, 1 (1964).
(41) E. A. Braude and E. A. Evans, *J. Chem. Soc.*, 3334 (1955).
(42) D. Heinert and A. E. Martell, *J. Am. Chem. Soc.*, **84**, 3257 (1962).
(43) H_0 values for HCl from E. M. Arnett and G. W. Mach, *J. Am. Chem. Soc.*, **88**, 1177 (1966).

Reactions in Moderately Concentrated Acids. 1.[1] A Novel Perspective in the Interpretation of Reaction Mechanisms

Vittorio Lucchini, Giorgio Modena,* Gianfranco Scorrano,* and Umberto Tonellato

Contribution from the Centro CNR Meccanismi di Reazioni Organiche, Istituto di Chimica Organica, Università di Padova, 35100 Padova, Italy.
Received May 3, 1976

Abstract: Equations to correlate rate constants with the acidity of the medium are derived from the hypothesis, already verified in protonation equilibria measurements, that linear free energy relationships exist between acidity functions. These equations require plotting against $(H_0 + \log [H^+])$ the quantity $\log k_\psi - \log ([SH^+]/[S]_{st})$, where the ratio $[SH^+]/[S]_{st}$ assumes different values depending on the basic strength of the substrate. The slope parameters obtained give information on the differences in solvation requirements on going from protonated substrates (strongly and moderately basic compounds) or from the substrate (weakly basic) in its free base form to the transition state. Information on the structure of the transition state may be inferred from the comparison of these solvation requirements with those observed in protonation equilibria studies. The hydrolysis rates of methyl *tert*-butyl ether, *tert*-butyl acetate, phenyl *tert*-butyl sulfoxide, and *N*-*tert*-butyl-2,4-dinitroaniline are reported as a function of the acid concentration and discussed, together with selected examples from the literature, in the light of the above treatment.

The field of equilibria and reactions in moderately concentrated aqueous solutions has attracted much attention by physical organic chemists both because of the challenging problems encountered and of the practical interest of acidic water as reaction solvent.[2-7] The interpretation of the results in this area has been largely based on the acidity function concept first proposed by Hammett and Deyrup[8] in 1932. Since then many aspects of the subject have been drastically revised mainly as a consequence of the observations made in recent years that (1) each class of bases, or at the limit of precision each base, follows its own acidity function;[9] (2) linear correlations exist between the various acidity functions.[10] Point 2 is of peculiar importance since it offers a means to reassess the entire field by choosing a single acidity function to which the acid–base behavior of any given compound can be related.

The equation[11] of choice (for reasons detailed elsewhere)[12] is that proposed by Bunnett and Olsen[10a,b] in the form suggested by Hammett:[10d]

$$H_S + \log [H^+] = (1 - \phi_c)(H_0 + \log [H^+]) \qquad (1)$$

Since $pK_{SH^+} = \log [SH^+]/[S] + H_S$, it follows from eq 1 that

$$\log ([SH^+]/[S]) + H_0 = \phi_c(H_0 + \log [H^+]) + pK_{SH^+} \qquad (2)$$

from which the pK_{SH^+} value of any given base may be evaluated.

The slope parameter ϕ_c is a measure of the solvation requirements of the species involved in the protonation equilibrium,[12-14] as may be appreciated by rewriting eq 1 in term of activity coefficients:[12-14]

$$\log f_{H^+} - \log (f_{SH^+}/f_S) = (1 - \phi_c)[\log f_{H^+} - \log (f_{BH^+}/f_B)] \qquad (3)$$

Indeed, since $f_{H^+} > f_{SH^+} > f_S$, positive ϕ_c values are to be expected for (f_{SH^+}/f_S) larger than (f_{BH^+}/f_B). Since $\log f$ is related to the free energy of transfer from water to the acid solution, a positive ϕ_c value implies a larger interaction of the solvent with the cation in the case of protonation of the base S than in the case of the Hammett base B. The ϕ_c values, which range from +1.0 to −1.6 and are tabulated elsewhere,[12,14] can be assembled according to the type of cation formed upon protonation. In fact, formation of oxonium ions requires[12] more positive ϕ_c values (e.g., for protonated alcohols $\phi_c = +0.85$ to +0.75) than formation of ammonium (0.0 to −0.4) and of carbonium (−0.7 to −1.6) ions. This finding was explained[12-15] in terms of a greater interaction of the solvent with the cation when this is small and the positive charge localized.[16]

The same approach may be applied to kinetic data of acid-catalyzed reactions to obtain information on the solvation, on the amount of charge localization, and hence on the structure of the transition state.

The rate equation for an acid-catalyzed reaction of the general type

$$S + H^+ \rightleftarrows SH^+ \rightarrow \ddagger \rightarrow \text{products} \qquad (4)$$